1
The Primary Organometallic in Copper-Catalyzed Reactions

Simon Woodward

1.1
Scope and Introduction

In this chapter, the term *primary organometallic* will mean both the terminal organometallic (RM) selected for a desired asymmetric transformation and those Cu-species that result once the RM is combined with a suitable copper precursor. A significant advantage in copper-promoted chemistry is the ability to access a very wide library of M[CuXR$\mathbf{L}_n$] species (M, main group metal; X, halide or pseudohalide; R, organofunction; **L**, neutral ligand) by simple variation of the admixed reaction components. Normally, the derived cuprate mixture is under rapid equilibrium such that if *one* species demonstrates a significant kinetic advantage, highly selective reactions can be realized. The corollary to this position is that deconvoluting the identity of such a single active species from the inevitable ''soups'' that result from practical preparative procedures can prove highly challenging. In this review, we concentrate on asymmetric catalytic systems developed in the last 10 years, but where necessary, look at evidence from simpler supporting achiral/racemic cuprates. Our aim is to try and present a general overview of bimetallic (chiral) cuprate structure and reactivity. However, given this extremely wide remit, the coverage herein is necessarily a selective subset from the personal perspective of the author. There are a number of past books of general use (either totally or in part) that provide good primers for this area [1]. Additionally, because of its relevance the reader is advised to also consult Chapter 12, which deals with mechanism.

Copper-Catalyzed Asymmetric Synthesis, First Edition.
Edited by Alexandre Alexakis, Norbert Krause, and Simon Woodward.

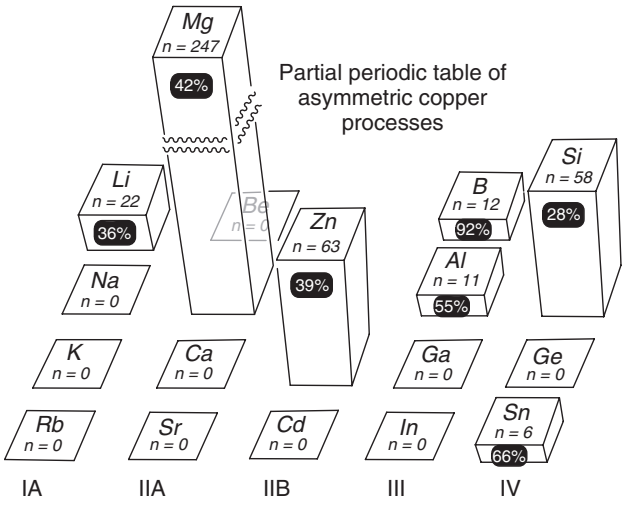

Figure 1.1 Approximate relative use (*n*) of group II–IV organometallics in copper-promoted asymmetric processes, and percentage increase of activity over 2007–mid 2012 (black roundels)[1)].

1.2
Terminal Organometallics Sources Available

One partial representation of the totality of asymmetric processes promoted by copper and main group organometallic mixtures is given in Figure 1.1; where the height of the bar indicates published activity (n = number of papers, etc.) and the percentage in the black roundel is the fraction published in the last 5 years (2007–2012).

The seven metals identified (Li, Mg, Zn, B, Al, Si, and Sn) form the basis of this overview. It should be noted that (i) the dominance of magnesium is due to numerous simple addition reactions where the resultant stereochemistry is controlled only by a chiral substrate; (ii) asymmetric reactions of the organometallics of the lower periods are still largely unreported; (iii) while all areas have developed, there has been especial interest in some metalloids in recent years (e.g., organoboron reactions); and (iv) the use of silicon organometallics is over reported in Figure 1.1 by the extensive use of silanes as reducing agents. The general properties of the organometallics used in asymmetric copper-promoted reactions are given in Table 1.1, compared with a generalized **L**CuR fragment. A common feature is their

1) The data arises from a Scifinder search (24 April 2012) of the terms: ''copper, asymmetric, and the various organoelement terms (e.g., organolithium, etc.).'' For Mg and Si, the more common terms *Grignard and silane* were used. Manual screening of the derived dataset indicated the applicability of the references to this chapter. A similar ratio of use was attained from substructure searching of asymmetric reactions of RM with generalized substrates.

Table 1.1 Properties of main group organometallics used in asymmetric Cu-promoted processes in order of element electronegativity.[a]

Organometallic type(s)	M–Me bond energy (kcal mol^{-1}) [kJ mol^{-1}]	M–C bond length (Å)	M–O bond energy (kcal mol^{-1}) [kJ mol^{-1}]	Electronegativity[b]		Oxophilicity[c]
LiR	64 [267]	2.31	112 [470]	0.98		1.7
RMgX, MgR_2	60 [253]	2.15	113 [471]	1.31	⇑ Transmetallation easier	2.3
AlR_3, AlR_nY_{3-n}	68 [283]	1.97	101 [418]	1.61		1.6
ZnR_2, RZnX	68 [285]	1.93	91 [381]	1.65		2.4
LCuR[d]	**57 [238]**	**1.98**	**49 [204]**	**1.90**		**0.7**
SiR_4, $R^1SiR^2{}_3$	77 [320]	1.85	100 [419]	1.90	⇓ Transmetallation harder	2.0
SnR_4, $R^1SnR^2{}_3$	63 [262]	2.16	49 [203]	1.96		1.0
BR_3, RBY_2	89 [374]	1.58	124 [519]	2.04		1.5

[a] Most data in Table 1 from Ref. [2], 1 kcal mol^{-1} is 4.19 kJ mol^{-1}; X = halide, Y = OR.
[b] Pauling's scale, data from Ref. [3].
[c] $E(M-O)/E(M-S)$ is often taken to correlate to a metal's oxophilic HSAB character, see Ref. [2].
[d] Generalized data from additional citations in Ref. [2].

tendency to form strong bonds with oxygen, providing strong thermodynamic driving forces for additions to carbonyl-containing substrates. This tendency can be correlated to their relatively low electronegativities and high oxophilicities (''hardness'' defined here as $E(M-O)/E(M-S)$]. The published Sn–O bond energy, derived from density functional theory (DFT) calculation, is probably somewhat underestimated in this respect. The reactivity of main group organometallics in Table 1.1 is reinforced by their weak M–C bonds. In fact, M–Me values are often upper limits – the bond energies of the higher homologs are frequently lower by 5–10 kcal mol^{-1} meaning that in mixed R^1MMe_n the methyls can be used as a potential nontransferable groups. Similarly, significant increases in the reactivity of organoelement compounds across the series M(alkyl), M(aryl), and M(allyl) are observed. At least in the allyl case, this is correlated to the M–C bond strength, which is typically >10 kcal mol^{-1} lower than M–Me.

1.3 Coordination Motifs in Asymmetric Copper Chemistry

Copper-promoted asymmetric reactions frequently attain high enantioselectivity through reduction in substrate conformational mobility via two-point binding, as in the general copper(I) cuprates **1a**,**b** or by η^2-binding at chiral Cu^{II} complexes, generalized by **2** (Scheme 1.1). As copper(II) does not form organometallic species, and readily undergoes reduction to Cu^{I} in the presence of RM, we concentrate here mainly on the former (overviews of activation by **2** can be found through the work

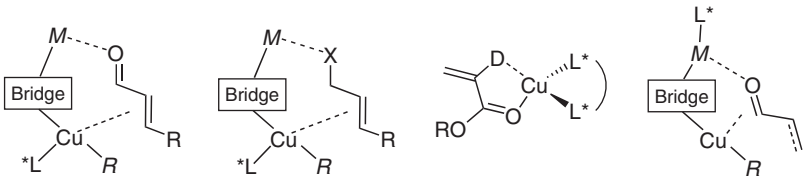

Scheme 1.1 Generalized binding modes for Cu-promoted activation of prochiral substrates where *MR* is a main group organometallic, X is a halogen, D is a generalized two electron donor, and ''bridge'' is a generalized anionic ligand. Extension to analogous isoelectronic fragments (e.g., NR for O, etc.) is, of course, possible.

of Rovis and Evans [4]). One other common scenario is use of a chiral Lewis acid fragment linked to a simple heterocuprate via a bridging ligand **3**.

Clearly, in attaining enantioselective transition states for asymmetric reactions, the nature of the bridging ligand (typically a halide or pseudohalide) is at least as important as the identification of an effective chiral ligand (**L***) in attaining effective docking of substrates in **1–3**.

1.3.1 Classical Cuprate Structure and Accepted Modes of Reaction

1.3.1.1 Conjugate Addition

Owing to their initial discovery, an enormous degree of activity has focused on the structures and reactivity of the Gillman-type homocuprates ($LiCuR_2$) and their heterocuprate analogs (LiRCuX, where X is the halide of pseudohalide [5]). In general, while these systems have provided underlying understanding of the basics of copper(I)/copper(III) organometallic chemistry they have *not* directly provided reagents that give highly selective *catalytic* asymmetric methodology. It is instructive to ask, ''Why is this the case?'' – a question that modern computational DFT understanding of the reaction course can cast light on. In classic conjugate addition, dimeric $[LiCuMe_2]_2$ reacts with cyclohexenone via transition state **4** [6], in which the enone-bound copper is formally at the +3 oxidation state (Scheme 1.2). One issue is that coordination of the d^8 Cu^{III} center with an additional neutral chiral ligand (e.g., a phosphine) has to compete with excess strong σ-ligands in the solution (e.g., Me^-), and also from intramolecular donation from the enolate π-bond (which renders the Cu-center coordinatively saturated). Another issue is associated with the lability of any $([R–Cu–R]Li)_n$ bridge. Although Li–O contacts in organocuprates are essentially covalent, an ionic formulation for **4** has been used here to emphasize the propensity of such units to exchange and associate. Such behavior is nicely demonstrated by the diffusion NMR studies of Gschwind [7], which measure the ''size'' of cuprates in solution allowing estimations of their identities. These studies show how easily cuprate-based bridges are readily displaced by tetrahydrofuran (THF) (leading to a catastrophic enone inactivation by loss of the $O_{enone}\cdots Li$ Lewis acid contact) or, alternatively, promotion of multiple

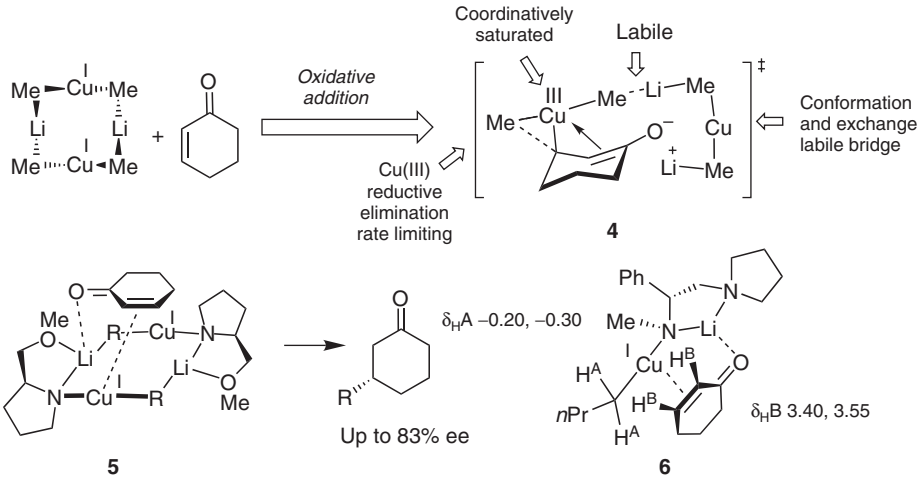

Scheme 1.2 Transition state issues and heterocuprate solutions in early reagent-controlled asymmetric syntheses.

species through aggregation of **4** in less polar solvents. This ease of displacement of homocuprate bridging groups by ''lithium-liking'' pseudohalides (e.g., alkoxide impurities in RLi or derived from halides in CuX precursors) sparked, even in the earliest days, ideas of avoiding such problems through heterocuprates LiRCuX* use (where X* provides a rigid ordered bridge promoting strong transfer of stereochemistry). The proposal of Dieter and Tokles **5** [8] (Scheme 1.2) is one such case. In fact, related species have been characterized in solution by NMR, of which **6** is a nice example [9].

Chiral heterocuprates of types **5** and **6**, and other species using alkoxide-based units, or related units controlling chirality through motif **3** (e.g., the sparteine-based reagents of Dieter [10]) have all provided rich structural chemistry [11] and effective asymmetric *stoichiometric* reagents for target synthesis [8, 10]. However, such chiral heterocuprate approaches have not transferred well to *catalytic* applications. Even the most effective system of van Koten [12] (Scheme 1.3) provides only a modest 76% ee_{max} in the addition of MeMgI to benzylidene acetone. This is not due to a failure in chiral recognition by the cuprate derived from **7** but due to unavoidable transfer of the chiral thiolate donor to the terminal main group RM source, which is facilitated by the excess of MeMgI present in the catalytic system. This provides inactive magnesium chiral thiolates and highly debilitating racemic catalysis through small amounts of $MgBr[CuMe_2]$. Davies *et al.* [13] has demonstrated an explicit case of the failure of a related ''nontransferable'' amido group in **8** as this undergoes rapid exchange on the NMR timescale leading, ultimately, to a mixture of homo and heterocuprates at 0 °C (Scheme 1.3).

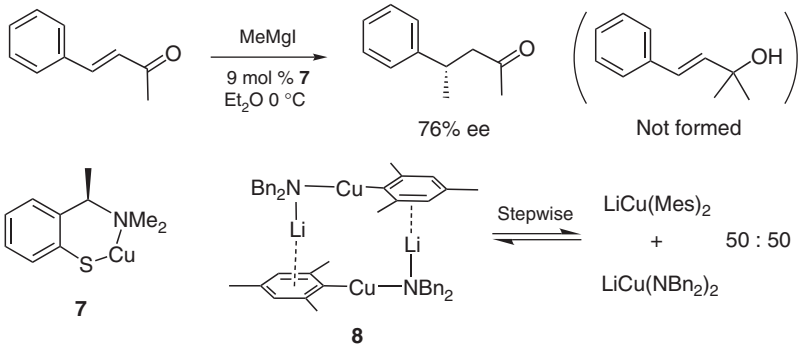

Scheme 1.3 Exchange of hetero groups in chiral heterocuprates and effects on selectivity.

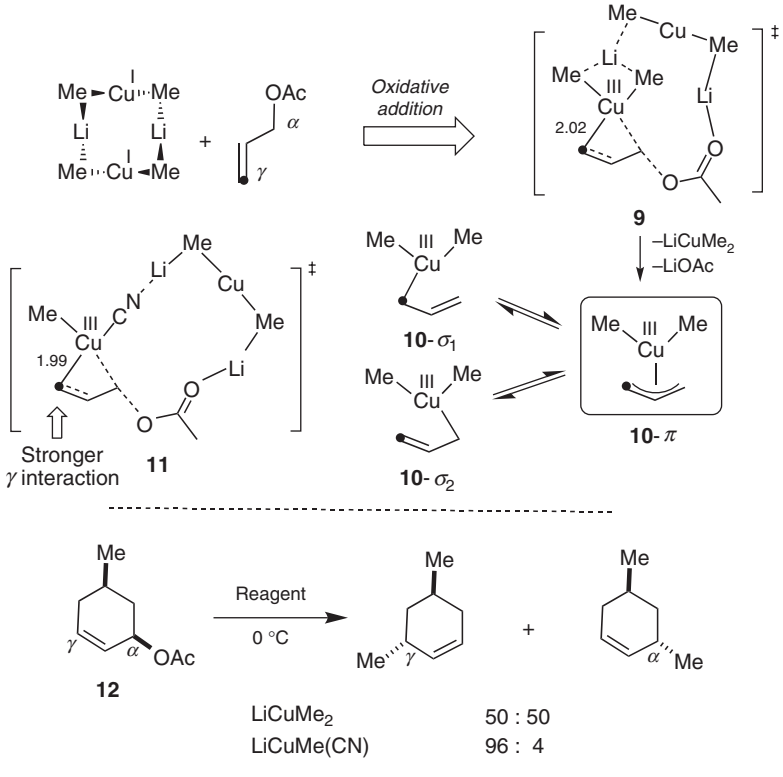

Scheme 1.4 DFT modeling of S_N2' allylation regiochemistry (key bond lengths in angstrom next to C_γ–Cu).

1.3.1.2 S_N2' Allylation Reactions

Despite early successes using chiral-leaving groups, before 1999 [14], Cu**L***-mediated asymmetric displacements of X (X = halide, OAc, $OP(O)(OEt)_2$, etc.) from (*E*)-$RCH{=}CHCH_2X$ proved highly challenging. While it was clear that the selective transition state(s) were normally associated with *anti* γ-attack of the nucleophile on allyl electrophile, the structures were rather too reactive to be identified. Using DFT approaches, Nakamura has put forward the most useful picture of the reaction coordinate (Scheme 1.4) [15]. Oxidative addition of allyl acetate to Gilman's reagent defines the enantioface of the electrophile coordinated and through transition state **9** and delivers the symmetrical π-allyl complex **10**. For clarity, the γ-carbon is emphasized (•). The symmetrical nature of **10-**π and its ability to undergo classic $\pi-\sigma$ interconversion indicates that, in substituted allylic systems, control of regiochemical issues is likely to be at least as great a challenge as inducing high levels of asymmetric selectivity. Support for these ideas comes from the interaction of theory and experiment. Replacing the $CuMe_2^-$ fragment by $MeCuCN^-$ in the DFT modeled oxidative addition reveals two factors: (i) a slower oxidative addition, but (ii) high polarization of the Cu d_{xz}-based highest occupied molecular orbital (HOMO) providing greater electron density trans to the CN group. This leads to more developed $C_\gamma-Cu$ bond in transition state **11**, which is retained in the resulting $Me(CN)Cu^{III}$ (allyl) intermediate (the analog of **10**). Faster reductive elimination of this species is also predicted, minimizing $\pi-\sigma$ interconversions. The predictions nicely account for the change of regioselectivity observed in the reactions of substrate **12** (Scheme 1.4).

1.3.2 Motifs in Copper-Main Group Bimetallics and Substrate Binding

The ground-state structures of active copper reagents, especially those ''loaded'' with reaction substrates, are normally too labile to be isolated. While major progress has clearly been made through computational (DFT) approaches above, scanning crystallographic databases[2)] reveals a significant number of model compounds that provide insight into substrate binding. For example, a handful of CuOTf complexes indicate similar binding modes for alkenes, dienes, and alkynes (all Cu–C 2.05–2.22 Å with C=C ~1.4 Å or C≡C ~1.2 Å), phosphines (Cu–P 2.19–2.28 Å), and triflate (Cu–O 2.04–2.43 Å). Particularly, structures OFANAK [16] and HIZCIC [17] provide tantalizing hints that typical bridging ligands such as triflate and acetate will produce highly ordered bimetallic structures when presented with suitable RM (Scheme 1.5). For example, in addition to clearly showing the poorer binding of the trisubstituted alkene, stripping out the core of OFANAK provides a key CuOTf core well predisposed to bind enones and RM. Similarly, HIZCIC

2) Search of the Cambridge Crystallographic database conducted (25 April 2012). The complexes analyzed were CAFQUV, CEJGEE, COMMAS, FUTRIV, GEKZOL, HIZCEY, HIZCIC, JUPXUN, MIMCAN, MOHLIE, OFANAK, REXJOU, TACYAX, and VIFSEJ.

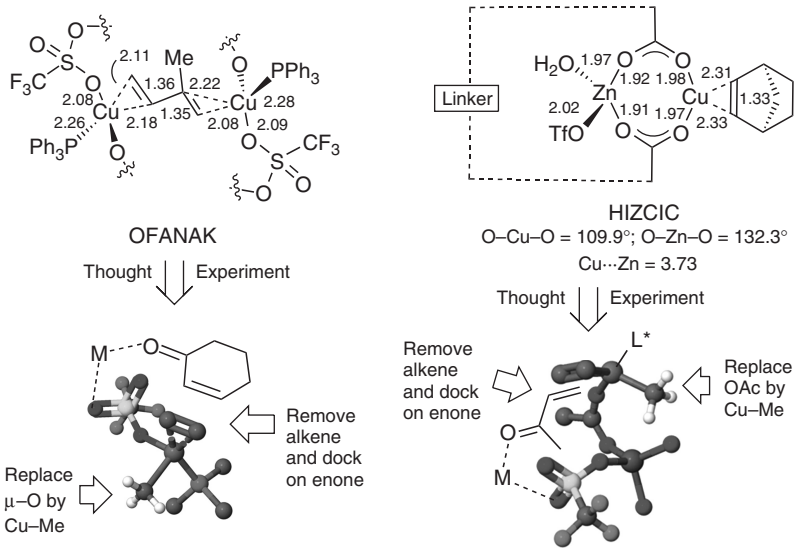

Scheme 1.5 Crystallographically characterized Cu(I) complexes as pointers to enone binding. Values next to bonds are interatomic distances in angstrom.

reveals the potentially tight and ordered structure that a bridging acetate can engender. For clarity, the $C_{40}H_{58}N_2O_4$ linker in HIZCIC is not shown. No structural data for carboxylate bridging between Cu^I and boron, aluminium, or silicon were found.

An additional range of X-ray structures are available providing insights into M-halide–Cu(I) motifs in nonisolable catalytic intermediates (M = Li, Mg, Zn, Si). These model compounds, together with selected inter Cu–X–M atomic distances are given in Scheme 1.6. In the case of Mg and Zn, only copper(II) models could be identified. By taking published average binding modes for the docking of carbonyl oxygen species with various main group metals [2] and a value of 2.15 Å for $Cu–C_{alkene}$ binding, then rough estimates of the optimal distance (d_2) the bridging ligand which should separate the Cu···M pair by for an *s-trans*-enone **13** (such as cyclohexenone), are attained (table in Scheme 1.6).

As can be seen, for the table within Scheme 1.6, single halogen atom bridges typically place the key M···Cu bimetallic pair a little closer than the idealized binding mode. It can be surmised that the success of larger bridging groups (OAc, OTf, thiophene carboxylate, etc.) in asymmetric catalysis is due to their ability to increase the Cu/M separation into an optimal range.

In the sections that follow, we focus on information that is available in real-world copper-based asymmetric reagents focusing on evidence that points to the structure of the primary cuprate (or other) species involved. In looking for common features, the reactivity has been grouped by metal rather than by transformation. Again,

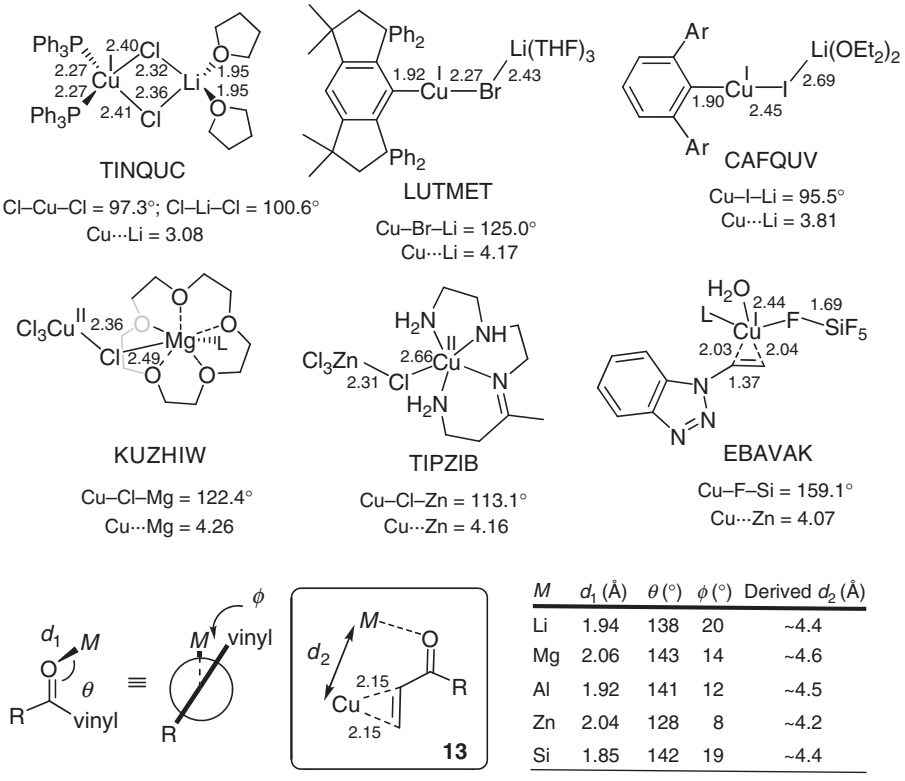

M	d_1 (Å)	θ (°)	ϕ (°)	Derived d_2 (Å)
Li	1.94	138	20	~4.4
Mg	2.06	143	14	~4.6
Al	1.92	141	12	~4.5
Zn	2.04	128	8	~4.2
Si	1.85	142	19	~4.4

Scheme 1.6 X-ray crystal structures of M–X–Cu model complexes (interatomic distances in angstrom) and their relationship to an idealized Cu···M bound *s-trans*-enone (d_2 calculated from J mol models).

a number of reviews, especially those concentrating on catalytic chemistry are pertinent [18].

1.4
Asymmetric Organolithium–Copper Reagents

Only very recently (2011) have organolithium reagents finally yielded to ligand-promoted asymmetric catalysis. Use of TaniaPhos $\mathbf{L_A}$ with CuBr·SMe_2 allows some utterly remarkable additions of alkyl organolithiums to (*E*)-cinnamyl bromides **14** (Scheme 1.7) with near perfect enantioselectivity [19]. This catalyst is able to promote the γ-selective allylation reaction with many desirable features: (i) ArBr exchange with *n*BuLi is avoided (run 3), (ii) alkyl substrates with poor steric profiles are tolerated (run 4), and (iii) even normal electrophiles for RLi (Boc groups and esters) are tolerated (run 6). The success of this chemistry is due to the

reaction conditions – RLi is added slowly into a very *nonpolar* solvent mix at low temperature. Under these conditions, only compound **16** is formed and this is stable to excess RLi in solution. The use of nonpolar solvent is critical. Replacement of CH_2Cl_2 by Et_2O results in the very fragile bimetallic **17** that readily expels the chiral ligand forming achiral $LiCuMe_2$, a process that can be followed by ^{31}P NMR spectroscopy. This decomposition pathway means that only low enantioselectivities are realized (28%) in Et_2O. In CH_2Cl_2–hexane, the ee values realized for *n*BuLi addition to **14** are largely independent of the copper source used ($CuBr{\cdot}SMe_2$, CuCl, CuI, Cu(TC); TC, 2-thiophene carboxylate), suggesting that this is a rare example of direct reaction of a ligated organocopper reagent (**17**) *without* a ligand bridge (halide or alkyl) to Li-activated **14** (cf. Scheme 1.4). This idea is supported by the observation that similar excellent behavior is achieved for hindered *i*Pr and *s*Bu additions to **14** (X = Cl) using a simple phosphoramidite ligand. Clearly, mechanistic and calculative studies are needed to address this point (Scheme 1.7).

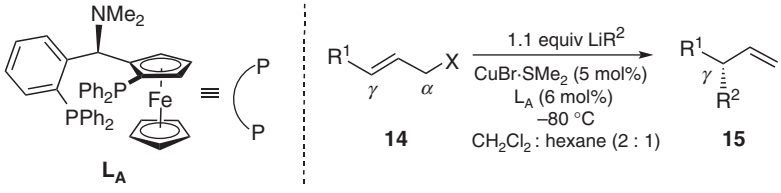

	X	R^1	R^2	Yield (%)	γ: α attack	ee (**15**)(%)
1	Br	Ph	Me[a]	90	90 : 10	99
2	Br	Ph	*n*Bu	88	90 : 10	99
3	Br	4-BrPh	*n*Bu	93	82 : 18	98
4	Br	nC_5H_{11}	Et	100[b]	94 : 6	95
5	Br	CH_2OBn	nC_6H_{13}	96	85 : 15	86
6	Br	OC(=O)Ph	*n*Bu	82	100 : 0	98

[a]In 2 : 1 CH_2Cl_2 : toluene for MeLi [b]Conversion

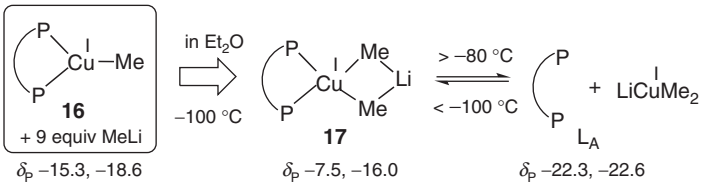

Scheme 1.7 Asymmetric S_N2' allylation with organolithium species.

The same simple phosphoramidite $\mathbf{L_B}$ has very recently allowed highly enantioselective desymmetrization reactions of exobicyclic alkenes (Scheme 1.8) [20]. However, in this case, no NMR studies were carried out on the primary organometallic, but clearly at least 1 equiv of Et_2O is tolerated by the catalyst structure.

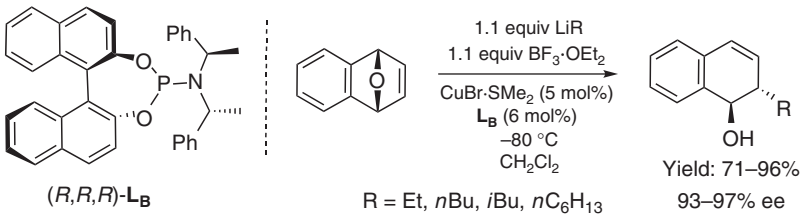

Scheme 1.8 Catalytic asymmetric desymmetrization of *meso*-bicyclic allylic epoxides.

1.5
Asymmetric Grignard–Copper Reagents

While traditional magnesium cuprates "$MgX[CuR_2]\cdot MgX_2$" are easily prepared by stoichiometric reaction of CuX with 2RMgX; extension to chiral heterocuprate versions of such chemistry have distinct limitations (see Section 1.1.1). The dramatic growth in this area in the last 10 years has come from utilization of chiral *diphosphine*-based copper(I) catalysts in nonpolar solvents, typically *t*BuOMe or CH_2Cl_2 [21], a concept whose genesis can be traced to the seminal use of *monophosphines* by Tomioka [22]. The primary organometallics involved in conjugate addition reactions have become unmasked through NMR studies. For example, the isolated Josiphos complex $[CuBrL_C]_2$ readily catalyzes the addition of a wide range of Grignard reagents to various α,β-unsaturated carbonyl compounds with good to excellent enantioselectivity (Scheme 1.9). Addition of excess MeMgBr to $[CuBrL_C]_2$ in CH_2Cl_2 led to formation of a major new species that was assigned structure **18** with a Cu–Me signal present at about δ_H −0.3, compared to the free

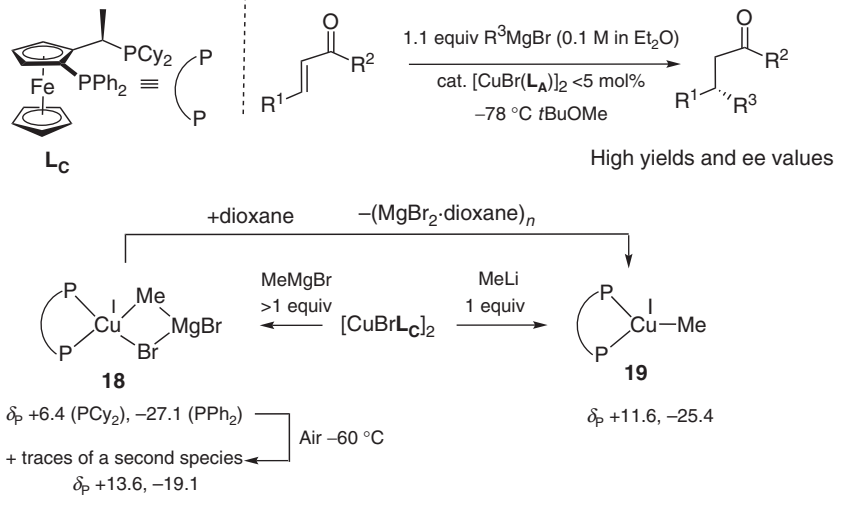

Scheme 1.9 Primary organometallics in conjugate additions promoted by Josiphos L_C.

Table 1.2 Primary organometallics in asymmetric 1,4 RMgX additions at about −60 °C.

Reaction conditions	Major species present
$CuBr{\cdot}SMe_2 + \mathbf{L_C} + MeMgBr$[a]	Mixture containing no **18**
$[CuBr\mathbf{L_C}]_2$ + excess MeMgBr (CH_2Cl_2, Et_2O, or toluene)	**18**
$[CuBr\mathbf{L_C}]_2$ + excess MeMgCl (CH_2Cl_2)	**19**
$[CuBr\mathbf{L_C}]_2$ + excess MeMgI (CH_2Cl_2)	Exchanging mixtures
$[CuBr\mathbf{L_C}]_2$ + excess MeMgBr (THF)	**19**
$[CuBr\mathbf{L_C}]_2$ + >2 equiv MeLi (CH_2Cl_2)	$\mathbf{L_C} + LiCuMe_2$

[a] Reaction solvent not defined.

MeMgBr at δ_H 1.64 [23]. The Cu:Me ratio in **18** was determined by integration of the methyl signal against the aryl region of the ligand. Traces of a second species were identified by ^{31}P NMR but its nature could not be ascertained; however, **18** was entirely converted to this entity when it was exposed to air at −60 °C. Conversely, when $[CuBr\mathbf{L_C}]_2$ was reacted with MeLi in CH_2Cl_2, only **19** was formed. The presence of $MgBr_2$ in **18** was confirmed by its precipitation as its dioxane coordination polymer. In stoichiometric reactions with (*E*)-BuCH=CHCOMe, each of the three species behave differently: **18** gives mostly 1,4-addition in 92% ee; **19** only traces of 1,4 addition in 62% ee; and the unknown species (δ_P +13.6, −19.1) 1,4-addition in 90% ee. In general, each of the species **18** and **19** is rather fragile and small changes in the reaction conditions dramatically change their populations, as can be seen in Table 1.2.

The rate of conjugate addition of RMgBr to Michael acceptors does not completely correlate to the concentration of **18** (specifically, its higher ethyl homolog) and this points to the involvement of a second species (as in the uncharacterized δ_P +13.6/−19.1 entity of Scheme 1.9). The presence of two cuprates in these Grignard-based systems is supported by the chemistry of Loh [24] (Scheme 1.10).

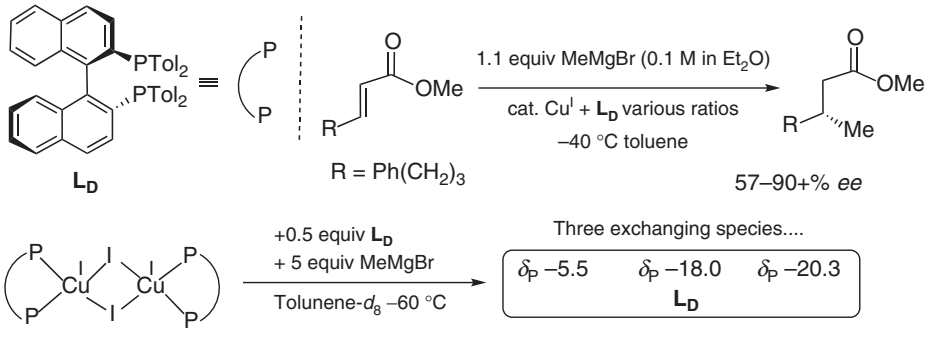

Scheme 1.10 Primary organometallics in conjugate additions promoted by (+)-2,2′-bis(di-*p*-tolylphosphino)-1,1′-binaphthyl (Tol-BINAP) $\mathbf{L_D}$.

Unfortunately, further structural data was not extractable from the ^{31}P NMR experiments – the signals in Loh's experiments are rather broad (such behavior is expected [25]) and no other nuclei were studied. On the basis of the (+)-ESI mass spectrum of the NMR sample, showing a cluster of isotopic peaks at around m/z 1445, the two species were assigned to ion-pairing isomers of the formula [Cu($\mathbf{L_D}$)$_2$][MgMeBrI]. However, this may be an artifact of the electrospray MS technique as such a latter complex is predicted to show m/z 1665 ($C_{97}H_{83}BrCuIMgP_4$) and the applicability of ESI-MS to sampling labile Mg/Cu organometallic systems has *not* been widely demonstrated. In contrast to the species of Feringa (**18** and **19**), it is clear that the catalytically competent primary organometallic must contain at least two $\mathbf{L_D}$ as the system shows a nonlinear product ee dependence when the ee of $\mathbf{L_D}$ is varied.

What the fate of the chiral-ligated cuprates in Scheme 1.9 and Scheme 1.10 is, after addition of suitable Michael acceptors, is unclear – no new compounds are detected in solution, which just begins generating enolate product. By analogy with Scheme 1.1 and Scheme 1.2, the presence of π-bound enone substrates and a transient Cu^{III} intermediate has been postulated. From a practical point of view, it is worth noting that equivalent additions of sp^2 (vinyl/aryl) Grignard reagents to enones have proved much more challenging for asymmetric catalysis suggesting a greater lability. Systems using moderately polar 2-methyl-THF and ligand $\mathbf{L_E}$ have proved the most effective (Scheme 1.11) but little is known about their intimate structure.

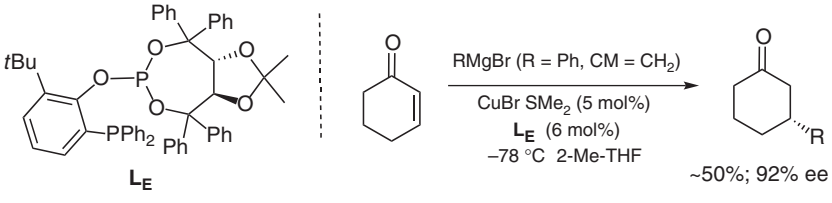

Scheme 1.11 1,4-Addition of sp^2 Grignards promoted by $\mathbf{L_E}$.

Similarly, while effective methods for catalytic asymmetric S_N2' allylation of RMgX reagents have recently become available [21], no attempts to reveal their exact primary structure through NMR has been successful thus far – again they appear highly labile. One clever approach to improving enantioselectivities is to build into the substrate a potential catalyst-directing group – an approach popularized by Breit and Schmidt [26]. However, using allylic dichloride **20** allows the product to retain a much more useful, and low mass, electrophilic site (Scheme 1.12) [27]. Coordination of one chloro group, either directly to Cu or via a magnesium bridge, orders the transition state derived from **21**, simultaneously delivering high enantioselectivity and *Z* selectivity in **22**. Falciola and Alexakis [28] have similarly proposed that a suitable (filled) ligand orbital stabilizes the Cu^{III} transition state **24** in selective transformation to **25** using the (*S*,*S*,*S*) diastereomer of $\mathbf{L_F}$ and other closely related ligands. The proposed interactions of Scheme 1.12 are closely akin to those discovered computationally in the cuprate **11** (Scheme 1.4).

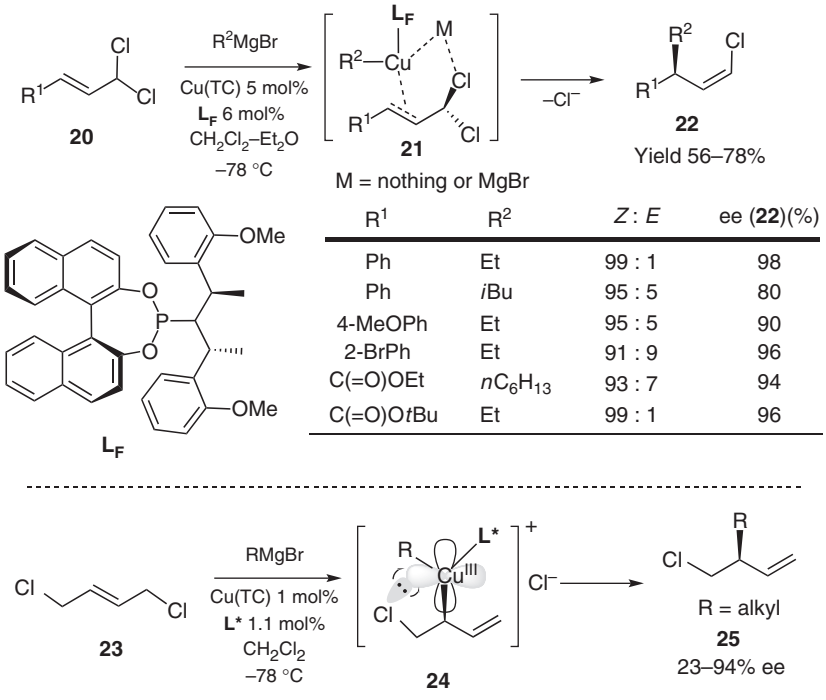

R^1	R^2	$Z:E$	ee (**22**)(%)
Ph	Et	99 : 1	98
Ph	*i*Bu	95 : 5	80
4-MeOPh	Et	95 : 5	90
2-BrPh	Et	91 : 9	96
C(=O)OEt	nC_6H_{13}	93 : 7	94
C(=O)O*t*Bu	Et	99 : 1	96

Scheme 1.12 Proposed direct (n → d) or MgX-bridged contact control in asymmetric S_N2' allylation reactions.

1.6 Asymmetric Organozinc–Copper Reagents

Although publications on asymmetric copper-catalyzed additions of organozinc reagents have become legion over the last 20 years, relatively few of these explicitly set out to probe the structure of the active copper reagent. Of the primary zinc organometallics, diorganozinc (ZnR_2) reagents are by far the most useful; the highly sluggish reactivity of organozinc halides (RZnX) limits their asymmetric applications in copper chemistry despite the early success of ''Knochel-type'' reagents (RZnCuCNX) [29]. While RZnX can be turned into more reactive ZnR_2 via Lewis acid-promoted Schlenk processes (Equation 1 and Equation 2, Scheme 1.13) [30] the presence of these additional promoters can cause problems – as in the formation of (±)-**26** during attempted asymmetric additions of BnZnBr. Nevertheless, such approaches can be moderately successful, as in BuZnCl minimization/activation in S_N2' chemistry (Scheme 1.13) [31].

Information on the nature of the organocopper species formed after transmetallation with ZnR_2 is not helped by the paucity of kinetic and NMR solution studies of such systems. In a seminal study, Noyori used ReactIR to obtain high quality kinetic data for $ZnEt_2$ 1,4-addition to enones promoted by very low levels of a 1 : 1

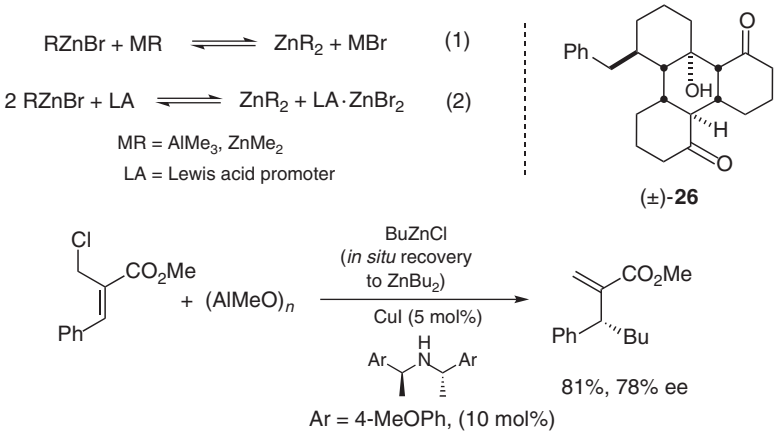

Scheme 1.13 Promoted zinc Schlenk equilibria processes as routes to diorganozincs.

mix of $PhSO_2NHBn$ and CuX (X = OTf, CN) [32]. This kinetic order dependence in this system is $[Cu{+}\mathbf{L}]^1[ZnEt_2]^1[enone]^1$ and the reaction was modeled by a rate law involving rapid preassociation of the components followed by rate-limiting conversion of an "activated complex" **27**. Unfortunately, supporting NMR data for **27** could not be attained. The unknown CuR_3Zn motif in **27** was assumed to be required to form a cuprate of sufficient reactivity for 1,4-insertion. Such analyses exclude any bridging ligand roles for triflate/cyanide – which could avoid the need for the unprecedented CuR_3Zn "higher order" cuprate in **27**. For example, structure **28** could equally be in accord with the kinetic data. In an asymmetric version of this chemistry (via modification of the sulfonamide ligand), Piarulli [33] determined the rate dependence of the components to be $[Cu{+}\mathbf{L}]^1[ZnEt_2]^0[enone]^1$, implying rapid transmetallation in this system. For more typical chiral PY_3 donors (phosphoramidites, phosphites), the exact composition of the organometallic resulting from mixtures of enone, ZnR_2, CuX, and used in asymmetric 1,4-additions is also contentious. Accurate kinetic data for these systems is notoriously hard to attain and the only published study fits almost equally well first- and second-order analyses of $[Cu_{cat}]$ and $[ZnEt_2]$ [5e, 34]. Direct NMR data of the "loaded" π-enone complexes is hard to attain owing to their high reactivity and the fast ligand exchange of Cu^I d^{10} centers. In the absence of direct evidence, proposals **29–31** have arisen (Scheme 1.14). Intermediate **29** has its origins in the original suggestion of Noyori that (fast) kinetic association of a second molecule of ZnR_2 is necessary to provide a cuprate of sufficient reactivity. Complex **31** has some supporting evidence based on diffusion-ordered NMR spectroscopy (DOSY) studies of the precatalytic mixtures of CuBr and $\mathbf{L_G}$ [35]. As the molecular volume of the complex is ligand dominated, the measured diffusion coefficients correlate to the number of ligands present. At 1 : 1 CuBr:$\mathbf{L_G}$ ratios, $(CuBr\mathbf{L_G})_3$ of unknown structure is present. At greater relative ligand concentrations (typically the Cu:**L** is 1 : > 1.5 in many asymmetric reactions), the tetrahedral–trigonal dimer $Cu_2Br_2(\mathbf{L_G})_3$ is formed (cf. **31**, Scheme 1.14) which

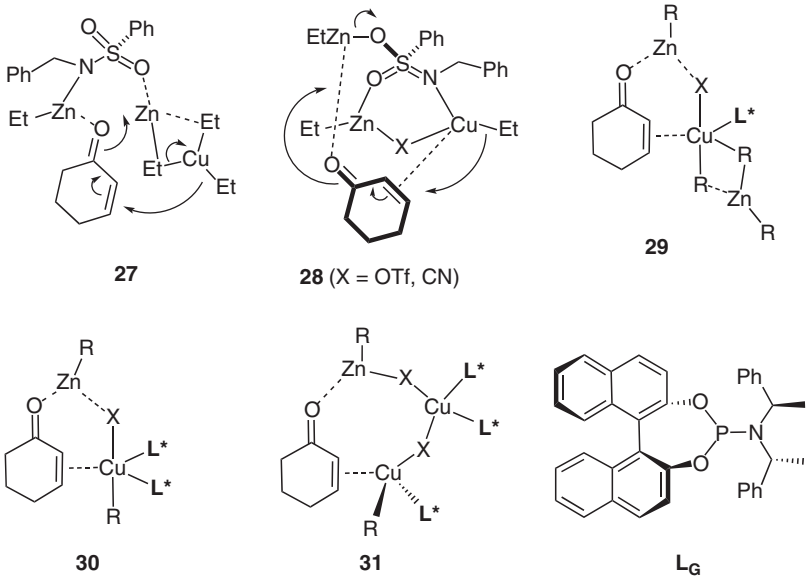

Scheme 1.14 Mechanistic proposals for active cuprate structure in conjugate addition of ZnR_2; **L*** is a generalized PY_3 donor, of which $\mathbf{L_G}$ is just one specific example.

is in equilibrium with other species via ligand association processes. The cleanest speciation was observed in $CDCl_3$, in more typical conjugate addition solvents (toluene, THF), a more complex mixture of exchanging complexes was formed. However, these DOSY studies have not yet been extended to real catalytic mixtures containing organometallics.

In the absence of direct experimental observation of enone π-complexes in this area, DFT computational studies have been carried out, which lend support to proposal **31**. A computationally less expensive PBE1PBE hybrid functional approach allows rapid *in silico* screening of the accessibility of **29–31**, among others, and this indicates that the latter is highly favored – much higher energy barriers to the formation of other species are encountered. In particular, computational attempts to attain the association of additional $ZnMe_2$ (i.e., motif **29**) failed – only facile dissociation of the zinc resulted. The reaction coordinate of the addition of $ZnMe_2$ to acetal-protected **32** was studied in detail and a viable transition state for the insertion of Cu–Me into the π-complex **33** was detected, whose calculated energy barrier was close to the experimentally observed value (Scheme 1.15) [36]. Interestingly, a closely related geometry has been calculated recently for (admittedly Cu-free) addition of $CH_2(ZnCl)_2$ to acrolein [37]. In copper-catalyzed asymmetric 1,4-additions of ZnR_2, most interest has focused on the screening of libraries of chiral ligands, of which huge ranges now exist [38]. However, owing to the bimetallic nature of the active catalyst, the nature of the bridging ligand may be at least as important to attaining high enantioselectivities, even though it is itself normally achiral. Evidence for this can be seen in the large range of ee values attained from

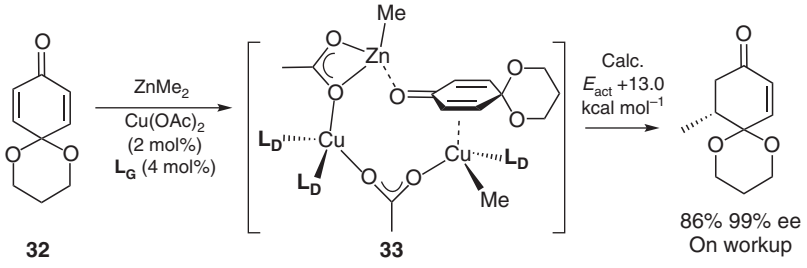

Scheme 1.15 A calculated π-complex in the 1,4-addition of $ZnMe_2$ to dienone **32**.

the same chiral ligand as a function of CuX precursor in $ZnEt_2$ additions in typical experimental optimizations [39]. Such effects become increasingly apparent when the potential bridging ligands are "built into" the fabric of the chiral ligand. Two instructive recent examples are the extended carboxylate in $\mathbf{L_H}$ [40], which allows stereocontrolled 1,6-additions (affording **34**); and $\mathbf{L_I}$, which allows enantiofacial reversal depending on the copper precursor used [41] (Scheme 1.16). While the structures of the key transition states in these reactions are not known, they clearly point to effects related to the structures of Scheme 1.5.

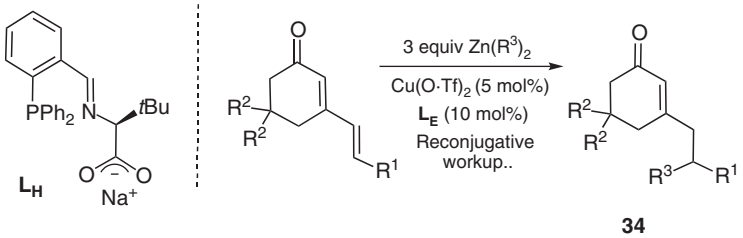

	R^1	R^2	R^3	Yield (%)	ee (**34**)(%)
1	Me	H	*n*Bu	79	97
2	Me	H	*i*Pr	71	97
3	*n*Bu	H	Et	63	95
4	Me	Me	Et	70	99
5	Me	Me	*n*Bu	75	86
6	Me	Me	*i*Pr	84	99

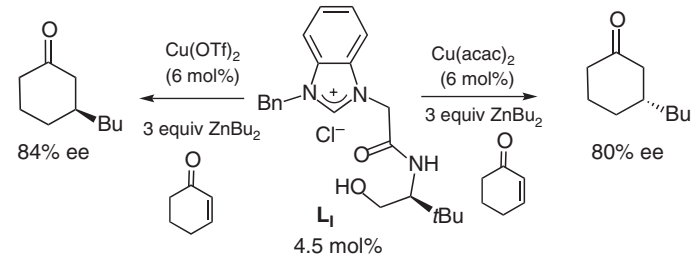

Scheme 1.16 Internal bridging ligand outcomes in ligands $\mathbf{L_H}$ and $\mathbf{L_I}$.

Direct experimental information on primary transmetallation events in S_N2' allylic substitution is sparse – mechanistic speculation being the norm. Through a series of chiral ligand modifications, Hoveyda was able to argue that reactive intermediates **35a**,**b** are responsible for the high enantioselectivity observed in γ-selective reaction of $ZnEt_2$ of allylic phosphates with his dipeptide-based ligands (Scheme 1.17). It is the terminal amide that plays the important organizational role – changing R from H to $CH^2C(O)OtBu$ in the initial amino acid has only a minor effect. The requirement for pseudohalide-to-copper bridging is not so clear cut in *N*-heterocyclic carbene (NHC)-based catalysts, while this has been proposed for noncopper systems [42]. Direct *stoichiometric* reaction of **36a** with enantiopure propargylic phosphates affords allenes with almost perfect chirality transfer to **37** [43]. Two points are of note: (i) racemization of the product allene **37** is minimal and (ii) in the published structures of isolated versions of such complexes, no indications of additional binding to the copper have been seen, the geometry being perfectly linear [44].

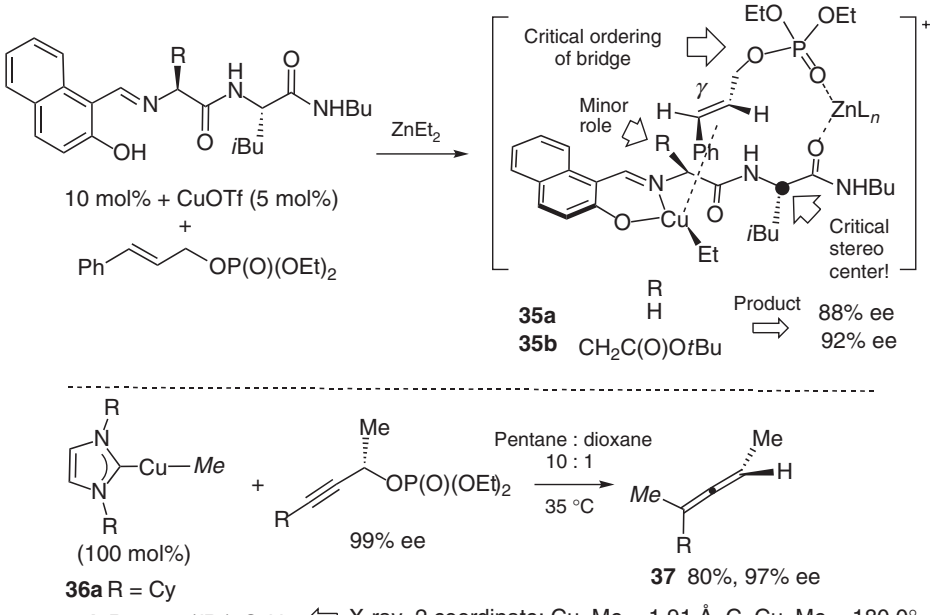

Scheme 1.17 Stereochemical observations in S_N2' allylations with peptidic and NHC-based ligands.

1.7
Asymmetric Organoboron–Copper Reagents

The widespread commercial availability of the pinacol-based diboron reagent (pin)B–B(pin) (pin = pinacolato = $OCMe_2CMe_2O$) since about 2005, has fostered

a meteoric rise in interest in asymmetric borylation due, in part, to the known utility of B–C bonds for further manipulation with retention of stereochemistry (e.g., oxidation and cross-coupling applications) [45]. The high strength of the B–O bond (Table 1.1) predicts that additions to carbonyls, Michael acceptors, and allylic electrophiles with oxy-leaving groups should all be favored, if electronegativity issues can be overcome in the transmetallation to copper (see Table 1.1). One successful strategy is the use of NHC ligands on copper, to obtain strongly stabilized Cu–B species, such as **38** (Scheme 1.18). These show remarkable stoichiometric transformations to stable (and, in many cases, crystallographically characterized) products, which, in many cases, can be rendered catalytic [46]. While this area is still in its infancy, asymmetric versions have been developed using chiral NHC ligands such as $\mathbf{L_J}$ that allows access to the equivalent Cu–B motifs (Scheme 1.18).

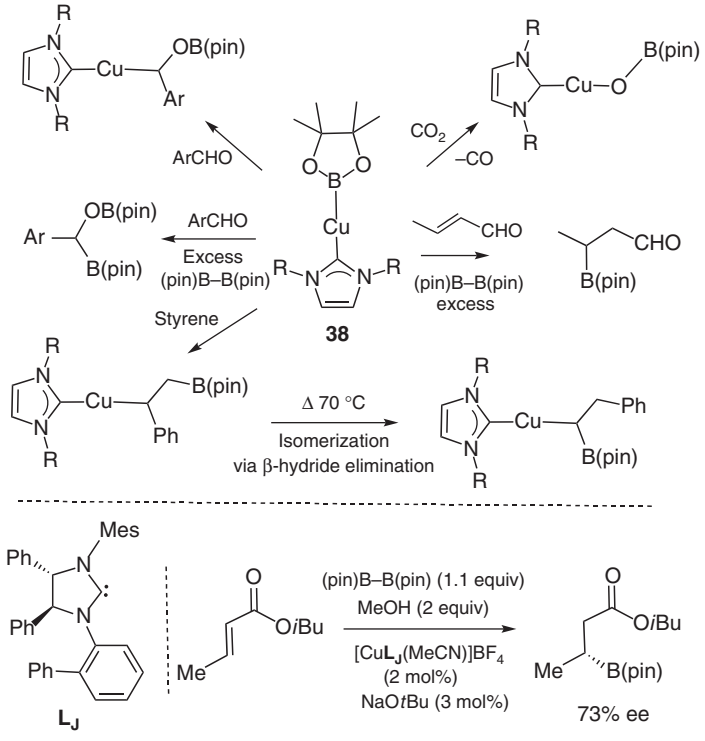

Scheme 1.18 Reactive entities in borylation reactions and associated catalytic processes.

The requirement for additional solvolytic alcohols or Lewis acids to attain catalytic turnover is a common feature of these processes – most notably in the work of Yun (use of ROH) and Shibasaki (use of *in situ* LiX) [45]. Similar approaches have been demonstrated [47]. DFT calculations provide insights on the need for these additives by indicating that the borylation of α,β-unsaturated substrates proceeds via

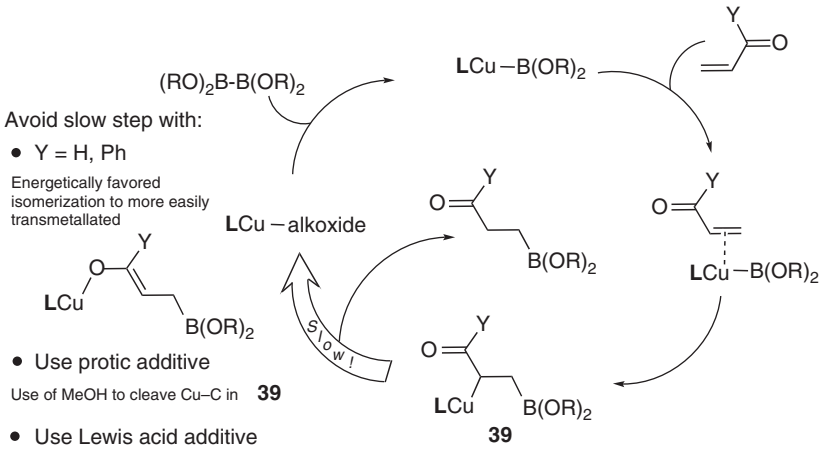

Scheme 1.19 Mechanistic pathways in borylation of α,β-unsaturated Michael acceptors.

borocupration, rather than direct 1,4-addition, affording **39** as the kinetically favored product due to the high B–C bond strength (about 85 kcal mol^{-1}) (Scheme 1.19) [48]. Conversion of the C-enolate **39** is rapid if Y = aryl, H but slow if Y = OR. Rapid protonolysis of **39** is given credence by the high deuterium incorporation observed in related experiments using MeOD [49] and by very recent studies demonstrating association of ROH with **39** by ESI-MS [50]. The Lewis acid promoters are thought to coordinate the carbonyl function of **39** activating it to transmetallation – but no theoretical study of this process has been made. The calculations of Scheme 1.19 were carried out with **L** = PMe_3 and these have not been repeated with the typical chiral ligands (e.g., $\mathbf{L_C}$) used in asymmetric catalysis. While computationally more expensive, such an approach would be useful in identifying potential key stereo-defining substrate–catalyst interactions.

Applications of (pin)B–B(pin) to asymmetric S_N2' allylation are also attractive as these directly provide allylboranes – classic stalwarts of asymmetric synthesis. Again, chiral diphosphines and NHC complexes have proved the most attractive promoters and both of these also provide clues into the nature of the primary organometallics. Recently, unprecedented *stereoconvergent* transformations of both acyclic and cyclic allylic ethers have been demonstrated (Scheme 1.20) [51]. The stereoconvergence of these reactions to single enantiomers with very high ee values is hard to explain by classic copper(III) π-allyl chemistry (cf. Scheme 1.4) that is expected to lead to observation of some α-coupled products, which is not the case. In light of the observations of Scheme 1.19, one alternative explanation is cuproboration via **40** and **42** leading to a transient σ-copper alkyl that then expels (pin)BOR on attack of the external diboron species. Such a mechanism would lead the selectivity to arise only through complexation of one π-face of the alkene avoiding the need for a range of different diastereomeric transition states to act kinetically very similarly. Finally, it is interesting to speculate if the features of

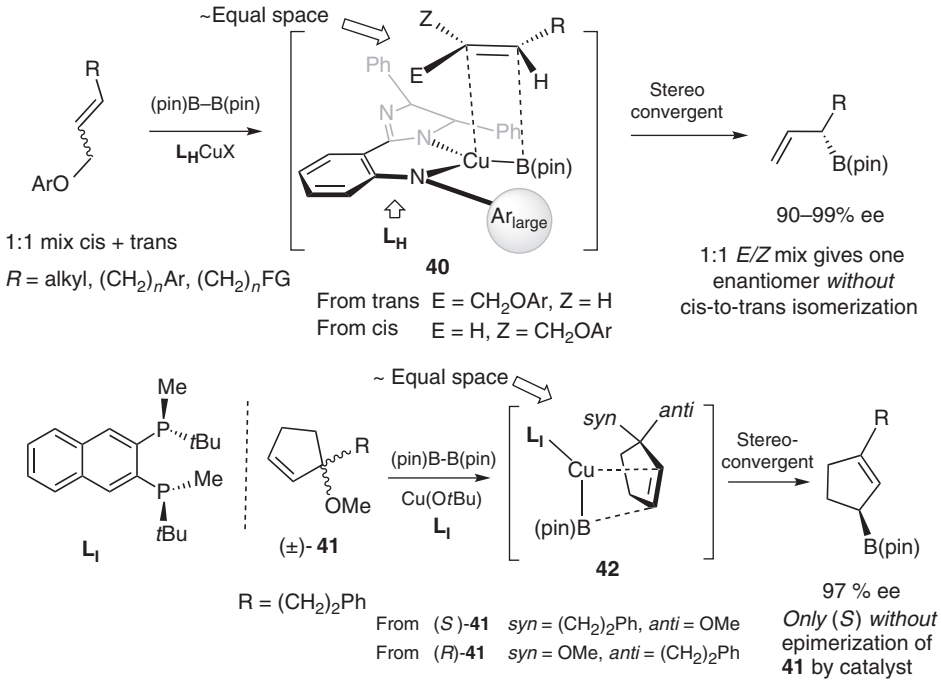

Scheme 1.20 Stereoconvergent substrate-binding modes in S_N2' borylation reactions.

Scheme 1.20 will extend into S_N2' additions of $ArB(OR)_2$ to allylic substrates for which good, nonasymmetric, precedents already exist [52].

1.8
Asymmetric Organoaluminium–Copper Reagents

Although alanes, AlR_3, have become recognized as some of the most effective terminal organometallics for asymmetric conjugate addition and S_N2' allylation strategies [53], information on the intimate structure of the primary organocopper species involved in these reactions is distinctly sparse. They are popularly assumed to be ''mechanistically analogous'' to additions of the equivalent diorganozinc reagents, yet there are significant differences – wildly differing enantiofacial selectivities; under near identical conditions to their zinc counterparts, the observation that the Cu^I source $[Cu(MeCN)_4]BF_4$ (which contains no strong ''bridging ligand'') is often effective points to the ''zinc-like'' analogy for Cu/Al systems being a poor one. Early low level PM3 studies on the rather too labile sulfide $\mathbf{L_K}$ has suggested structures **43** and **44** for the major π-enone precursor and conjugate addition pathway (Scheme 1.21) [54] but this ligand is unrepresentative of most of the ''modern'' generation.

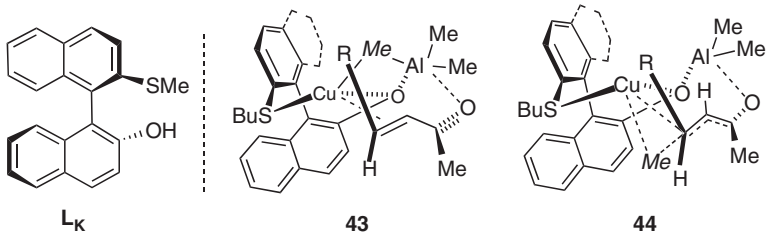

Scheme 1.21 PM3-derived primary organometallics in Cu^{I}/L_J-catalyzed conjugate addition to linear enones.

Some definitively characterized Cu–R species have been prepared via organoaluminium reagents (Scheme 1.22). Significantly, air-sensitive **45** has been characterized both in solution and crystallographically [45a, 55] and these are of clear relevance to organoalane 1,4 and S_N2' reactions catalyzed by chiral NHC complexes. The B3LYP/6-31G(d) calculated bond dissociation energy (BDE) of the Cu–Me in **45** is ~80 kcal mol^{-1}. The high oxophilicity of AlR_3 reagents can cause problems with ligand stability. For example, phosphoramidites coordinate $AlMe_3$ in nonpolar toluene or CH_2Cl_2 leading to adducts of type **46** and rapid cleavage to **47** (Scheme 1.22) [56]. Related processes in NHC chemistry are known, as in the formation of **48**, but this is slow (20 h) and less likely to compete in the presence of Cu(I) sources [42].

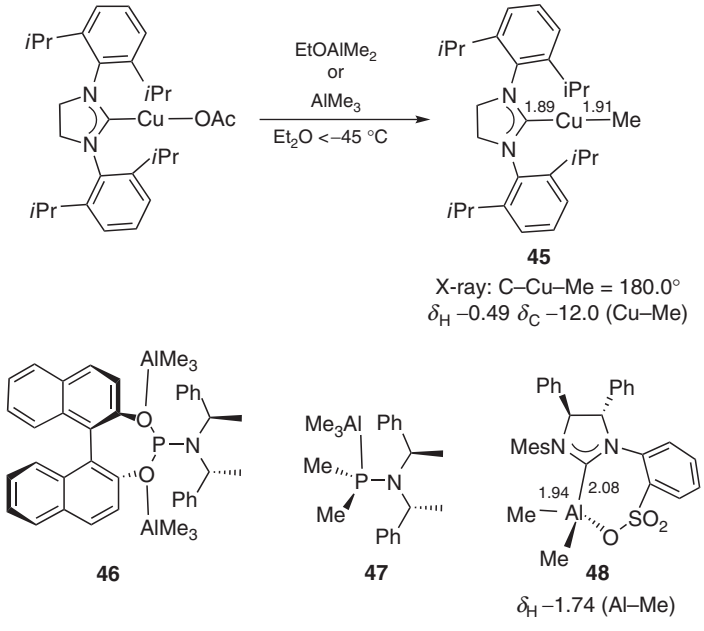

Scheme 1.22 $AlMe_3$-promoted transmetallations; bond distances for **45** and **48** in angstrom.

Finally, it is important to realize that, the role of bridging ligands in asymmetric cuprates, while recognized as important, is not very well understood. Thus, although simple examples of such motifs are well characterized – as in the crystal structures of XARDUR and XARFON (Scheme 1.23) extrapolation to predicted selective asymmetric intermediate, such as **49**, is presently just mechanistic speculation and further computational and spectroscopic studies are sorely needed here.

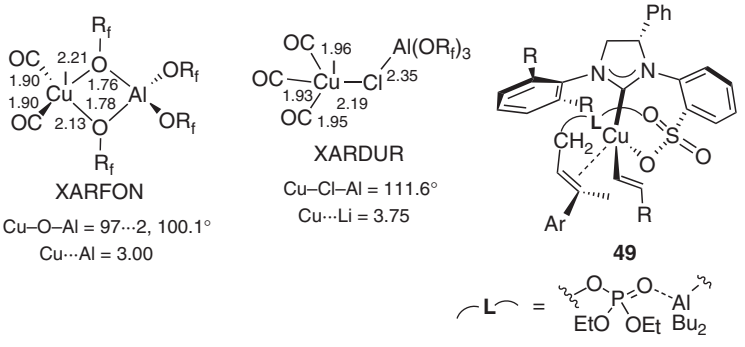

Scheme 1.23 Bridging ligand roles; distances in angstrom.

1.9
Asymmetric Silane and Stannane Copper-Promoted Reagents

Organosilane reagents engage in a wide range of copper-catalyzed transformations of enones, allylic(pseudo)halides, and carbonyl compounds via primary organometallics of the types: **L**CuR, **L**CuH, and **L**CuSiR_3. While the majority of the asymmetric processes that have arisen use chiral phosphines to produce the desired induction, the intermediates in such reactions have proved too labile to allow study. Conversely, NHC species (although mostly achiral) allow insights into structure and reactivity. Scheme 1.24 shows crystallographically characterized examples derived from (NHC)CuX transmetallation with appropriate organosilanes [57]. Direct comparison of their Cu–C_α electron density via their ^{13}C NMR spectra is unfortunately not possible as this was only provided for **52**. The formation of the latter may be a good model for similar processes occurring in the catalytic enone reduction chemistry of Lipshutz and Krause [58] (Scheme 1.24). The presence of (*n*-octyl)SiF_3 is vital for effective catalysis, but how this aids transmetallation is presently unknown. Similarly, **50** directly enters into catalytic 1,2-additions to aldehydes and is therefore clearly related to imine 1,2 allylation, of which formation of **53** is a nice example [59].

Recent contributions have been made in understanding of asymmetric reductions of carbonyl compounds. These reactions are believed to involve initial formation of a chiral copper hydride that inserts into the C=O bond to deliver a product alkoxide

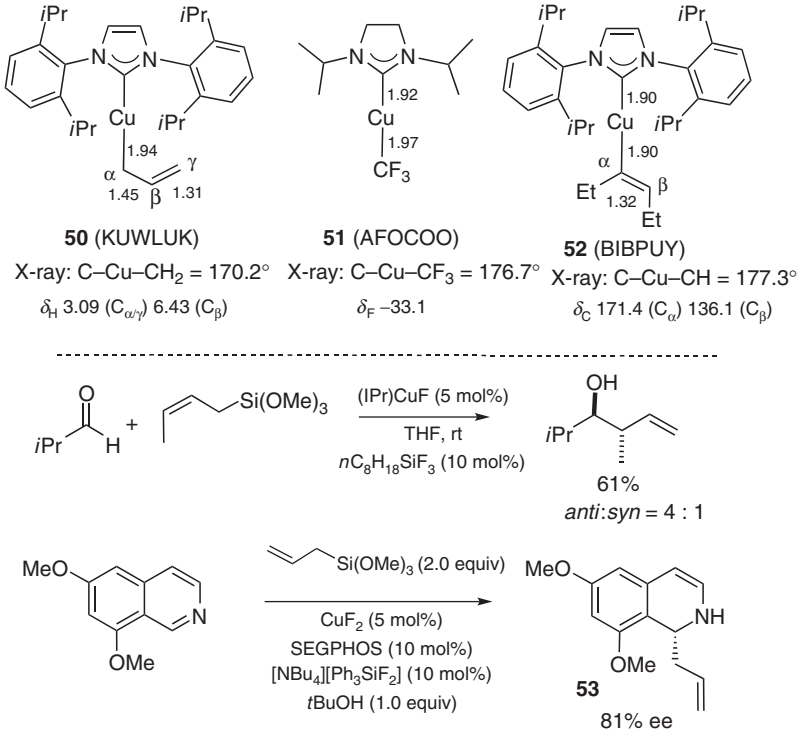

Scheme 1.24 Organocopper species via transmetallation from Y_3Si-R and applications; **50** ex. (allyl)$Si(OMe)_3$, **51** ex. $TMSCF_3$, **52** ex. EtCCEt and $HSiEt_3$. Distances in angstrom.

that then undergoes transmetallation to close the catalytic cycle (Scheme 1.25). DFT modeling of this proposed pathway suggests that the rate determining step for the process is transmetallation of copper alkoxide intermediate. The absence of any nonlinear effect (NLE) in the product ee when scalemic mixtures of a chiral ligand are used point strongly to mononuclear catalysis. However, kinetic analysis of the reaction of acetophenone and Ph_2SiH_2, under CuCl/NaO*t*Bu/1,1′-binaphthyl (BINAP) catalysis yields the component dependency: $[\text{ketone}]^1[\text{silane}]^1[\text{CuL}]^{0.5}$. The half dependence in catalyst concentration is believed to indicate that the resting state of the catalyst is the copper dimer **54** [60]. Very recently an example (2011, structure INIRIH) of such a species has been characterized where the bridging hydrides were crystallographically located [61]. The cycle of Scheme 1.25 is also in accord with recent (2011) studies using C_2-chiral NHC ligands [62]. Two further interesting facts are (i) the calculated energy barriers for the cleavage of the initial mononuclear alkoxide are unexpectedly high and (ii) that test stoichiometric reactions of LCuH species, in the absence of excess silane, fail. Kleeberg *et al.* [63] has explicitly characterized **55**, which results from (NHC)Cu-$SiMe_2Ph$ addition to TolCHO. This undergoes slow cleavage with (pin)B-$SiMe_2Ph$ to give the equivalent silyl product.

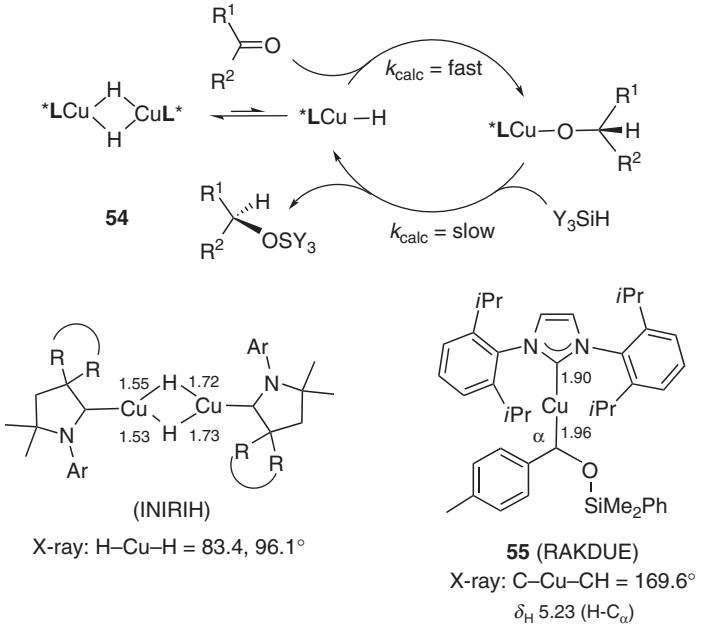

Scheme 1.25 Copper hydride involvement in asymmetric ketone reduction; distances in angstrom.

Until comparatively recently copper-catalyzed 1,4- and S_N2' additions of Cu-SiR_3 have resisted attempts to render them efficient asymmetric processes. In essence the issue is that the generalized asymmetric copper(I) silyl **56** must compete against ligand free silyl cuprates or other main group silyl anions for addition to the substrate (Scheme 1.26) [18k]. The latter species are easily formed in even slightly

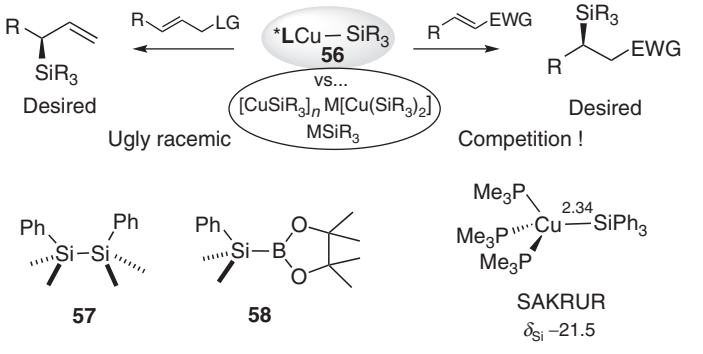

Scheme 1.26 Competition in transmetallation in asymmetric silylation; distances in angstrom.

''ionizing'' reaction mixtures and their rates of addition are comparable (or even better!) than addition of most examples of **56**. Successful solutions to this problem center around use of the reagents $PhMe_2Si\text{-}SiMe_2Ph$ **57** and $PhMe_2Si\text{-}B(pin)$ **58** to afford clean transmetallation to **56** with the formation of only covalent (non promoting) by-products. A simple model for **56** is available in crystallographically characterized SAKRUR, which was attained from the reaction of CuCl, PMe_3, and Ph_3SiLi in early work [64]. Once the restrictions of Scheme 1.26 were realized, then ligand screening soon revealed a range of chiral phosphines and NHC ligands able to deliver good to excellent levels of enantioselectivity for conjugate 1,4-additions (for details see Ref. [18k]).

The situation is even more problematic in S_N2' allylation chemistry. While transmetallation to copper from a variety of ''R_3Si^-'' sources is facile, Oestreich has shown that facile $\sigma-\pi-\sigma$ interconversion occurs in allylcopper species derived from $Zn(SiPhMe_2)_2$, containing LiCl, leading to rapid erosion of and induced stereochemistry [65]. While use of reagent **58** allows effective ''ligand free'' systems for silylation of (*E*)-cinnamyl chloride type allylic electrophiles, the use of BINAP or Josiphos ligated equivalents gave only low conversions to racemic products [66].

Well characterized species involved in cuprostannation remain essentially unreported, apart from the $(IPr)CuSnPh_3$ complex of Sadighi which shows an almost linear $C_{NHC}-Cu-Sn$ motif with a Cu–Sn bond distance of 2.47 Å [67]. This species shows a strong tendency to react with EX electrophiles fashioning EPh and $SnPh_2$. The relationship of such isolated complexes to tin-based enantioselective catalysis largely remains to be defined. For example, in the reaction of allylstannanes with 2-nitrosopyridine no transmetallation to copper(I) is proposed, the latter acting only as a Lewis acid [68].

1.10 Conclusions

Even within the short space of this overview, it is clearly seen that, while the intimate structures of the primary organometallics present in enantioselective cuprate reagents are becoming better defined, a very wide range of factors can perturb their constitutions. In particular, the simplest reaction parameter – the solvent, can have a profound effect in directing the chiral cuprate from simple ligated organocopper species to complex bridged structures containing a wide range of gegenion Lewis acids.[3)] Controlling such effects for effective asymmetric catalysis requires a mixture of ''discovery'' and ''design'' approaches [54].

3) The author is indebted to his coworkers past and present for input into this document and to Dr Ross Denton (University of Nottingham) for DFT calculations on CuXMe (X = O, S).

References

1. Principal textbooks of relevance: (a) Perlmutter, P. (1992) *Conjugate Addition Reactions in Organic Synthesis*, Pergamon, Oxford; (b) Taylor, R.J.K. (ed.) (1994) *Organocopper Reagents, a Practical Approach*, Oxford University Press, Oxford; (c) Krause, N. (ed.) (2002) *Modern Organocopper Chemistry*, Wiley-VCH Verlag GmbH, Weinheim; (d) Rappoport, Z.Z. and Marek, I. (eds) (2009) *The Chemistry of Organocopper Compounds Parts 1 and 2*, Wiley-VCH Verlag GmbH, Weinheim; (e) Córdova, A. (2010) *Catalytic Asymmetric Conjugate Reactions*, Wiley-VCH Verlag GmbH, Weinheim.
2. Most data from: (a) Woodward, S. (2002) *Tetrahedron*, **58**, 1017–1050 For the generalised **L**CuR data see: structures ESOXAL and JAXSIK in the Cambridge Crystallographic database (Cu–Me distances); (b) Ziegler, T., Tschinke, V., and Becke, A. (1987) *J. Am. Chem. Soc.*, **109**, 1351–1358 (Cu–Me bond energy). The bond enthalpies for CuYMe (Y = O gives 48.8 kcal mol^{-1}; Y = S gives 72.8 kcal mol^{-1}) were calculated by the same DFT methods used for the other metals.
3. Pauling, L. (1960) *The Nature of the Chemical Bond*, 3rd edn, Cornell University Press, Ithaca, NY.
4. For a comparison of the approaches of Scheme 1 see: Rovis, T. and Evans, D.A. (2001) *Prog. Inorg. Chem.*, **50**, 1–150.
5. For useful introductory overviews of this area see: (a) Woodward, S. (2000) *Chem. Soc. Rev.*, **29**, 393–401; (b) Nakamura, E. and Mori, S. (2000) *Angew. Chem. Int. Ed.*, **39**, 3750–3771; (c) Mori, S. and Nakamura, E. (2002) in *Modern Organocopper Chemistry Parts 1 and 2* (ed. N. Krause) Chapter 10, Wiley-VCH Verlag GmbH, Weinheim, pp. 315–345; (d) Nakamura, E. and Yoshikai, N. (2009) in *The Chemistry of Organocopper Compounds Parts 1 and 2* (eds Z.Z. Rappoport and I. Marek) Chapter 1, Wiley-VCH Verlag GmbH, Weinheim, pp. 1–21; (e) Woodward, S. and Willcox, D. (2012) Ligated organocuprates: an A-Z routemap of mechanism and application, in *Innovative Catalysis in Organic Synthesis* (ed. P.G. Andersson), Wiley-VCH Verlag GmbH, Weinheim.
6. (a) Mori, S. and Nakamura, E. (2002) *Modern Organocopper Chemistry*, Chapter 10, Wiley-VCH Verlag GmbH, Weinheim, pp. 315–345; (b) Mori, S. and Nakamura, E. (1999) *Chem. Eur. J.*, **5**, 1534–1543.
7. For an overview see: Gschwind, R. (2008) *Chem. Rev.*, **108**, 3029–3053 especially Sections 3.2-3.3.
8. For a summary of such early approaches see: Rossiter, B.E. and Swingle, N.M. (1992) *Chem. Rev.*, **92**, 771–806.
9. Eriksson, J. and Davidsson, Ö. (2001) *Organometallics*, **20**, 4763–4765.
10. (a) Dieter, R.K., Topping, C.M., Chandupatla, K.R., and Lu, K. (2001) *J. Am. Chem. Soc.*, **123**, 5132–5133; (b) Dieter, R.K. and Chen, N. (2006) *J. Org. Chem.*, **71**, 5674–5678.
11. (a) Kronenburg, C.M.P., Amijs, C.H.M., Jastrzebski, J.T.B.H., Lutz, M., Spek, A.L., and van Koten, G. (2002) *Organometallics*, **21**, 4662–4671; (b) Lang, H., Leschke, M., Mayer, H.A., Melter, M., Weber, C., Rheinwald, G., Walter, O., and Huttner, G. (2001) *Inorg. Chim. Acta*, **324**, 266–272.
12. Arink, A.M., Braam, T.W., Keeris, R., Jastrzebski, J.T.B.H., Benheim, C., Rosset, S., Alexakis, A., and van Koten, G. (2004) *Org. Lett.*, **6**, 1959–1962 and references therein.
13. (a) Davies, R.P., Hornauer, S., and Hitchcock, P.B. (2007) *Angew. Chem. Int. Ed.*, **46**, 5191–5194; (b) Bomparola, R., Davies, R.P., Hornauer, S., and White, A.J.P. (2009) *Dalton Trans.*, 1104–1106.
14. Dübner, F. and Knochel, P. (1999) *Angew. Chem. Int. Ed.*, **38**, 379–381.
15. Yoshikai, N., Zhang, S.L., and Nakamura, E. (2008) *J. Am. Chem. Soc.*, **130**, 12862–12863.
16. Håkansson, M., Brantin, K., and Jagner, S. (2000) *J. Organomet. Chem.*, **602**, 5–14.
17. LeCloux, D.D., Davydov, R., and Lippard, S.J. (1998) *Inorg. Chem.*, **37**, 6814–6826.

18. Overviews of the development of recent asymmetric catalytic methodology: (a) Harutyunyan, S.H., den Hartog, T., Geurts, K., Minnaard, A.J., and Feringa, B.L. (2008) *Chem. Rev.*, **108**, 2824–2852 (covers Mg systems). (b) Alexakis, A., Bäckvall, J.E., Krause, N., Pàmies, O., and Diéguez, M. (2008) *Chem. Rev.*, **108**, 2796–2823 (covers Al, Mg, Zn and other systems); (c) Deutsch, C., Krause, N., and Lipshutz, B.H. (2008) *Chem. Rev.*, **108**, 2916–2927 (covers Si-H systems); (d) von Zezschwitz, P. (2008) *Synthesis*, **2008**, 1809–1831 (covers Al systems); (e) Yamada, K. and Tomioka, K. (2008) *Chem. Rev.*, **108**, 2874–2886 (ZnR 1,2-additions); (f) Shibasaki, M. and Kanai, M. (2008) *Chem. Rev.*, **108**, 2853–2873 (1,2-additions to C=O); (g) Thaler, T. and Knochel, P. (2009) *Angew. Chem. Int. Ed.*, **48**, 645–648 (covers Mg, Zn systems); (h) Falciola, C.A. and Alexakis, A. (2008) *Eur. J. Org. Chem.*, 3765–3780 (covers S_N2' chemistry); (i) Jerphagnon, T., Pizzuti, M.G., Minnaard, A.J., and Feringa, B.L. (2009) *Chem. Soc. Rev.*, **38**, 1039–1075 (covers ligands and mechanism); (j) Schiffner, J.A., Müther, K., and Oestreich, M. (2010) *Angew. Chem. Int. Ed.*, **49**, 1194–1196 (covers B systems); (k) Hartmann, E., Vyas, D.J., and Oestreich, M. (2011) *Chem. Commun.*, **47**, 7917–7932 (B and Si systems).
19. (a) Pérez, M., Fañanás-Mastral, M., Bos, P.H., Rudolph, A., Harutyunyan, S.R., and Feringa, B.L. (2011) *Nat. Chem.*, **3**, 377–381; (b) Fañanás-Mastral, M., Pérez, M., Bos, P.H., Rudolph, A., Harutyunyan, S.R., and Feringa, B.L. (2012) *Angew. Chem. Int. Ed.*, **51**, 1922–1925.
20. Bos, P.H., Rudolph, A., Pérez, M., Fañanás-Mastral, M., Harutyunyan, S.R., and Feringa, B.L. (2012) *Chem. Commun.*, **48**, 1748–1750.
21. For an overview of this area see: reference 18a.
22. (a) Kanai, M. and Tomioka, K. (1995) *Tetrahedron Lett.*, **36**, 4275–4278; (b) Kanai, M., Nakagawa, Y., and Tomioka, K. (1999) *Tetrahedron*, **55**, 3843–3854.
23. Harutyunyan, S.R., López, F., Browne, W.R., Correa, A., Peña, D., Badorrey, R., Meetsma, A., Minnaard, A.J., and Feringa, B.L. (2006) *J. Am. Chem. Soc.*, **128**, 9103–9118.
24. (a) Wang, S.Y., Ji, S.J., and Loh, T.P. (2007) *J. Am. Chem. Soc.*, **129**, 276–277; (b) Wang, S.Y., Song, P., and Loh, T.P. (2010) *Adv. Synth. Catal.*, **352**, 3185–3189.
25. Black, J.R., Levason, W., Spicer, M.D., and Webster, M. (1993) *J. Chem. Soc., Dalton Trans.*, 3129–3136.
26. Overview: Breit, B. and Schmidt, Y. (2008) *Chem. Rev.*, **108**, 2928–2951.
27. Giannerini, M., Fañanás-Mastral, M., and Feringa, B.L. (2012) *J. Am. Chem. Soc.*, **134**, 4108–4111.
28. Falciola, C.A. and Alexakis, A. (2008) *Chem. Eur. J.*, **14**, 10615–10627.
29. Knochel, P. and Jones, P. (eds) (1999) *Organozinc Reagents, A Practical Approach*, Oxford University Press, Oxford.
30. Blake, A.J., Shannon, J., Stephens, J.C., and Woodward, S. (2007) *Chem. Eur. J.*, **13**, 2462–2472.
31. Goldsmith, P. and Woodward, S. (2005) *Angew. Chem. Int. Ed.*, **44**, 2235–2237.
32. Masato Kitamura, M., Miki, T., Nakano, K., and Noyori, R. (2000) *Bull. Chem. Soc. Jpn.*, **73**, 999–1014.
33. Gallo, E., Ragaini, F., Biello, L., Cenini, S., Gennari, C., and Piarulli, U. (2004) *J. Organomet. Chem.*, **689**, 2169–2176.
34. Pfretzschner, T., Kleemann, L., Janza, B., Harms, K., and Schrader, T. (2004) *Chem. Eur. J.*, **10**, 6048–6057.
35. A significant range of other precatalytic conditions has also been studied this way: (a) Zhang, H. and Gschwind, R.M. (2006) *Angew. Chem. Int. Ed.*, **45**, 6391–6394; (b) Schober, K., Zhang, H., and Gschwind, R.M. (2008) *J. Am. Chem. Soc.*, **130**, 12310–12317; (c) Zhang, H. and Gschwind, R. (2007) *Chem. Eur. J.*, **13**, 6691–6700.
36. Welker, M., Woodward, S., Veiros, L.F., and Calhorda, M.J. (2010) *Chem. Eur. J.*, **16**, 5620–5629.
37. Sada, M., Furuyama, T., Komagawa, S., Uchiyama, M., and Matsubara, S. (2010) *Chem. Eur. J.*, **16**, 10474–10481.
38. See for example Alexakis, A. and Benhaim, C. (2002) *Eur. J. Org. Chem.*, 3221–3236 and references therein.

39. Alexakis, A., Benhaim, C., Rosset, S., and Humam, M. (2002) *J. Am. Chem. Soc.*, **124**, 5262–5263.
40. Wencel-Delord, J., Alexakis, A., Crévisy, C., and Mauduit, M. (2010) *Org. Lett.*, **12**, 4335–4337.
41. Shibata, N., Okamoto, M., Yamamoto, Y., and Sakaguchi, S. (2010) *J. Org. Chem.*, **75**, 5707–5715.
42. Lee, Y., Li, B., and Hoveyda, A.H. (2009) *J. Am. Chem. Soc.*, **131**, 11625–11633.
43. Uehling, M.R., Marionni, S.T., and Lalic, G. (2012) *Org. Lett.*, **14**, 362–365.
44. (a) Mankad, N.P., Gray, T.G., Laitar, D.S., and Sadighi, J.P. (2004) *Organometallics*, **23**, 1191–1193; Care must be taken in extension of this idea to catalytic systems as aggregation effects have precedent in some cases, see: (b) Díez-González, S., Escudero-Adán, E.C., Benet-Buchholz, J., Stevens, E.D., Slawin, A.M., and Nolan, S.P. (2010) *Dalton Trans*, **39**, 7595–7606.
45. For an overview see reference 18j and references therein.
46. (a) Laitar, D.S., Müller, P., and Sadighi, J.P. (2005) *J. Am. Chem. Soc.*, **127**, 17196–17197; (b) Laitar, D.S., Tsui, E.Y., and Sadighi, J.P. (2006) *J. Am. Chem. Soc.*, **128**, 11036–11037; (c) Laiter, D.S., Tsui, E.Y., and Sadighi, J.P. (2006) *Organometallics*, **25**, 2405–2408; (d) Bonet, A., Lillo, V., Ramirez, J., Fernandez, E., and Diaz-Requejo, M.M. (2009) *Org. Biomol. Chem.*, **7**, 1533–1535.
47. Selected recent developments: (a) Hong, B., Ma, Y., Zhao, L., Duan, W., He, F., and Song, C. (2011) *Tetrahedron: Asymmetry*, **22**, 1055–1062; (b) Ibrahem, I., Breistein, P., and Cordova, A. (2011) *Angew. Chem. Int. Ed.*, **50**, 12036–12041; (c) Gao, M., Thorpe, S.B., Slebodnick, C., Santos, W.L., Kleeberg, C., and Marder, T.B. (2011) *J. Org. Chem.*, **76**, 3997–4007.
48. Dang, L., Lin, Z., and Marder, T.B. (2008) *Organometallics*, **27**, 4443–4454.
49. Yamamoto, Y., Kirai, N., and Harada, Y. (2008) *Chem. Commun.*, 2010–2012.
50. Pubill-Ulldemolins, C., Bonet, A., Gulyas, H., Fernández, E., and Bo, C. (2012) *Chem. Eur. J.*, **18**, 1121–1126.
51. (a) Park, J.K., Lackey, H.H., Ondrusek, B.A., and McQuade, D.T. (2011) *J. Am. Chem. Soc.*, **133**, 2410–2413; (b) Ito, H., Kunii, S., and Sawamura, M. (2010) *Nat. Chem.*, **2**, 972–976.
52. (a) Whittacker, A.M., Rucker, R.P., and Lalic, G. (2010) *Org. Lett.*, **14**, 3216–3218; (b) Ohmiya, H., Yokokawa, N., and Sawamura, M. (2010) *Org. Lett.*, **12**, 2438–2440.
53. The latest (at 2012) summary of this area is in the *Topics in Organometallic Chemistry series*: Pàmies, O. and Diéguez, M. (2012) Conjugate addition of organoaluminium species to michael acceptors and related processes, in *Modern Organoaluminium Reagents: Preparation, Structure, Reactivity and Use* (eds S. Dagorne and S. Woodward), Springer, New York.
54. Woodward, S. (2007) *Synlett*, 1490–1500.
55. Goj, L.A., Blue, E.D., Delp, S.A., Gunnoe, T.B., Cundari, T.R., Pierpont, A.W., Petersen, J.L., and Boyle, P.D. (2006) *Inorg. Chem.*, **45**, 9032–9045.
56. Bournaud, C., Falciola, C.A., Lecourt, T., Rosset, S., Alexakis, A., and Micouin, L. (2006) *Org. Lett.*, **8**, 3581–3584.
57. (a) Russo, V., Herron, J.R., and Ball, Z.T. (2010) *Org. Lett.*, **12**, 220–223; (b) Dubinina, G.G., Furutachi, H., and Vicic, D.A. (2008) *J. Am. Chem. Soc.*, **130**, 8600–8601; (c) Mankad, N.P., Laitar, D.S., and Sadighi, J.P. (2004) *Organometallics*, **23**, 3369–3371.
58. See reference 18c for an overview. For recent developments see: Voigtritter, K.R., Isley, N.A., Moser, R., Aue, D.H., and Lipshutz, B.H. (2012) *Tetrahedron*, **68**, 3410–3416 (DFT calculations on 1,2 vs 1,4 modes).
59. Miyazaki, M., Ando, N., Sugai, K., Seito, Y., Fukuoka, H., Kanemitsu, T., Nagata, K., Odanaka, Y., Nakamura, K.T., and Itoh, T. (2011) *J. Org. Chem.*, **76**, 534–542.
60. (a) Issenhuth, J.T., Notter, F.P., Dagorne, S., Dedieu, A., and Bellemin-Laponnaz, S. (2010) *Eur. J. Inorg. Chem.*, 529–541; (b) Zhang, W., Li, W., and Qin, S. (2012) *Org. Biomol. Chem.*, **10**, 597–604.

61. Frey, G.D., Donnadieu, B., Soleihavoup, M., and Bertrand, G. (2011) *Chem. Asian J.*, **6**, 402–405.

62. Albright, A. and Gawley, R.E. (2011) *J. Am. Chem. Soc.*, **133**, 19680–19683.

63. Kleeberg, C., Feldmann, E., Hartmann, E., Vyas, D.J., and Oestreich, M. (2011) *Chem. Eur. J.*, **17**, 13538–13543.

64. Cowley, A.H., Elkins, T.M., Jones, R.A., and Nunn, C.M. (1988) *Angew. Chem., Int. Ed Engl.*, **27**, 1349–1350.

65. (a) Schmidtmann, E.S. and Oestreich, M. (2006) *Chem. Commun.*, 3643–3645; (b) Vyas, D.J. and Oestreich, M. (2010) *Chem. Commun.*, **46**, 568–570.

66. Vyas, D.J. and Oestreich, M. (2010) *Angew. Chem. Int. Ed.*, **49**, 8513–8515.

67. Bhattacharyya, K.X., Akana, J.A., Laitar, D.S., Berlin, J.M., and Sadighi, J.P. (2008) *Organometallics*, **27**, 2682–2684.

68. Chatterjee, I., Fröhlich, R., and Studer, A. (2011) *Angew. Chem. Int. Ed.*, **50**, 11257–11260.